PERGAMON

Journal of the Mechanics and Physics of Solids
49 (2001) 1847–1864

JOURNAL OF THE
MECHANICS AND
PHYSICS OF SOLIDS

www.elsevier.com/locate/jmps

Delamination of compressed films on curved substrates

John W. Hutchinson*

Division of Engineering and Applied Sciences, Harvard University, Cambridge, MA 02138, USA

Abstract

Delamination is considered for thin elastic films that are bonded to cylindrical substrates and subject to an equi-biaxial compressive pre-stress. Results for both positive and negative curvatures are obtained. The film buckles or deflects (depending on the sign of the curvature) away from the substrate inducing mixed mode stress intensities at the edge of the delamination. The energy release rate and combination of modal stress intensities at the delamination edges are determined. Steady-state propagation of delamination blisters is analyzed for both axial and circumferential propagation directions. The results depend strongly on the substrate curvature. Circumferential propagation is suppressed when the curvature is negative, but is favored when the curvature is positive. Axial propagation can occur for both positive and negative curvature substrates.
© 2001 Elsevier Science Ltd. All rights reserved.

Keywords: A. Delamination; Thin films; B. Residual stress; A. Fracture mechanics; Curved substrates

1. Introduction

Films under inplane compression that are bonded to flat substrates can undergo buckling-driven delamination when the combination of film thickness and stress exceeds a critical value. Curvature of the substrate can enhance or suppress delamination, depending on the sign of the curvature and the direction of propagation. In this paper, results for the steady-state propagation of delamination blisters on cylindrical substrates will be determined. The steady-state results form the basis for robust criteria which ensure delaminations will not spread. Delaminations are a primary failure

* Tel.: +1-617-495-2848; fax: +1-617-495-9837.
E-mail address: hutchinson@husm.harvard.edu (J.W. Hutchinson).

0022-5096/01/$ - see front matter © 2001 Elsevier Science Ltd. All rights reserved.
PII: S0022-5096(01)00029-1

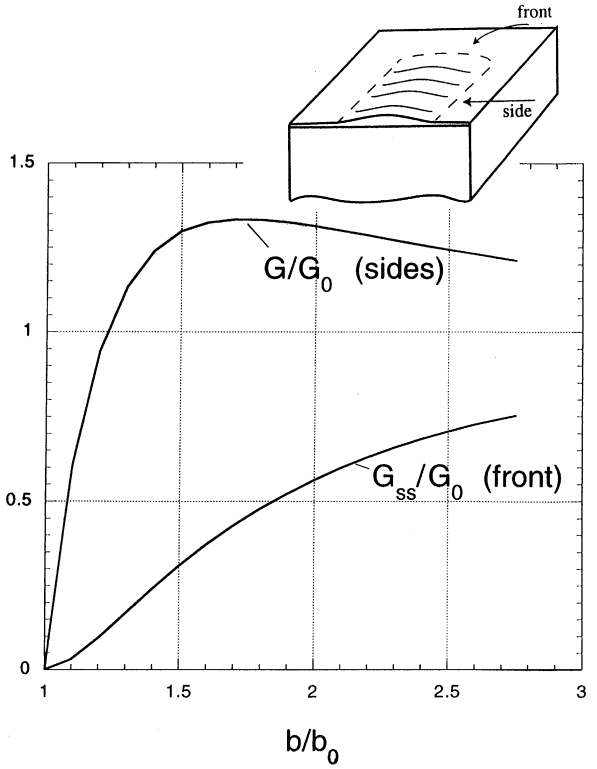

Fig. 1. Energy release rates on the sides and curved front of a straight-sided blister on a flat substrate.

mechanism for oxide films on wire heating elements and for ceramic thermal barrier coatings on turbine engine blades and other hot section components. Both applications involve curved substrates.

We begin by reviewing the rationale behind the tendency for buckle-driven delaminations on flat substrates to grow at their curved front while their sides remain stationary. This behavior is manifest in the propagation of a straight-sided blister (Fig. 1) and the so-called telephone cord blister. The film is modeled as a flat plate that is clamped along its edges (Chai et al., 1981; Evans and Hutchinson, 1984; Hutchinson et al., 1992; Giola and Ortiz, 1997; Nilsson et al., 1993; Nilsson and Giannakopoulos, 1995). The energy release rate and the mix of modes I and II stress intensity factors of the interface crack can be obtained with the aid of a basic elasticity solution for a film on a substrate acted on by an edge moment and inplane force (Hutchinson and Suo, 1992). The energy release rate on the sides of the straight-sided blister well behind the curved front is

$$\frac{G}{G_0} = \left(1 - \left(\frac{b_0}{b}\right)^2\right)\left(1 + 3\left(\frac{b_0}{b}\right)^2\right), \tag{1}$$

where

$$G_0 = \frac{1-\nu^2}{2}\frac{\sigma_0^2 t}{E}, \tag{2}$$

with σ_0 as the uniform equi-biaxial compressive stress in the unbuckled film, t the film thickness, and E and ν as the film's Young's modulus and Poisson's ratio, respectively. In Eq. (1), b is the half-width of the blister and b_0 is the value of the half-width at which the onset of buckling will occur at the pre-stress σ_0:

$$b_0 = t\frac{\pi}{\sqrt{12(1-\nu^2)}}\sqrt{\frac{E}{\sigma_0}}. \tag{3}$$

The steady-state energy release rate averaged over the curved front of the straight-sided blister is

$$\frac{G_{ss}}{G_0} = \left(1-\left(\frac{b_0}{b}\right)^2\right)^2. \tag{4}$$

The two energy release rates are plotted in Fig. 1 where it is clearly seen that the energy release rate along the sides significantly exceeds that along the curved front. Nevertheless, once a straight-sided blister has formed, propagation is observed to occur along its front with no further advance along its sides. How is this possible? The reason rests with the different mode mixities along the sides and front, coupled with the strong dependence of the toughness of most interfaces on the mixity.

The mode mixity, $\psi = \tan^{-1}(K_{II}/K_I)$, associated with the sides and the front are plotted in Fig. 2. These apply to the case where there is no elastic mismatch between the film and the substrate, but the mismatch effect is not large unless the moduli differences are extreme. The results for the sides is exact (Hutchinson and Suo, 1992), while that for the curved end is approximated by using the result for a circular blister with the same radius b and energy release rate $G = G_{ss}$. The curves are terminated at the value of b/b_0 at which the sides attain pure mode II conditions. It is evident that, at a given width, b, the sides have a siginificantly larger proportion of mode II to mode I than the curved front. One can understand this physically in that buckling along the sides enables the film to undergo an inplane displacement away from the edge, while such motion is much more constrained along the curved front. The inplane displacement contributes significantly to the mode II component of intensity. This is the essence of the difference between a straight and curved front.

A phenomenological interface toughness law which reflects the strong mode dependence observed for some interfaces is (Hutchinson and Suo, 1992)

$$\Gamma_i(\psi) = \Gamma_i^{(1)}(1+\tan^2(1-\lambda)\psi), \tag{5}$$

where $\Gamma_i(\psi)$ is the interface toughness and mode mix ψ, $\Gamma_i^{(1)}$ is the mode I toughness for $\psi = 0$, and λ is a parameter that adjusts the mode dependence. If $\lambda = 1$, there is no mode dependence. Representative values for many interfaces appear to lie in the range $\lambda \leqslant 0.3$. The ratio of the mode II ($\psi \pm 90^\circ$) to mode I toughness is $1+\tan^2(1-\lambda)\pi/2$, which is 4.85 for $\lambda = 0.3$.

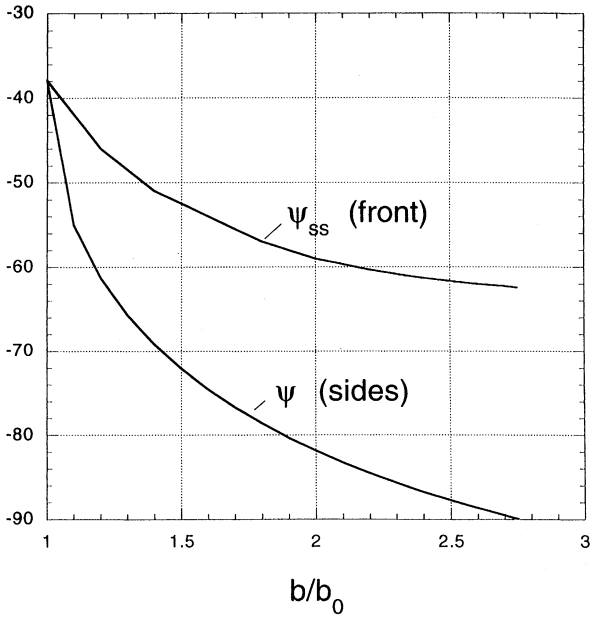

Fig. 2. Measure (in degrees) of the relative amount of mode II–I on the sides and curved front of a straight-sided blister on a flat substrate.

For the sides, the propagation condition can be stated as $G = \Gamma_i(\psi)$ or, equivalently, as $F \equiv G/(1+\tan^2(1-\lambda)\psi) = \Gamma_i^{(1)}$. Similarly, the condition for propagation along the front is $F_{ss} \equiv G_{ss}/(1+\tan^2(1-\lambda)\psi_{ss}) = \Gamma_i^{(1)}$. The ratio of the mode-adjusted energy release rates,

$$\frac{F_{ss}}{F} = \frac{G_{ss}/(1+\tan^2(1-\lambda)\psi_{ss})}{G/(1+\tan^2(1-\lambda)\psi)}, \tag{6}$$

measures the tendency to propagate at the front or on the sides: if it is greater than 1 propagation along the front is favored, and vice versa. This ratio is plotted in Fig. 3 for several values of λ. If there is no mode dependence of the interface toughness ($\lambda = 1$), propagation will always occur on the sides, implying straight-sided blisters could not exist. However, when there is substantial interface toughness mode dependence, propagation at the front is favored for blisters above a critical size. The fascinating morphological shapes of buckle-driven delaminations derive from this coupling of buckling nonlinearity with interfacial fracture mode dependence.

Motivated by the above discussion, our treatment of delamination on cylindrical substrates will emphasize the energy release rate and mode mixity on both the sides and the front of straight-sided delamination blisters. These results are obtained from the analysis of a one dimensional problem characterizing behavior well behind the front. We begin by giving two simple results which provide some insight into aspects of the behavior. Then, in Section 3, delaminations propagating axially along a cylindrical

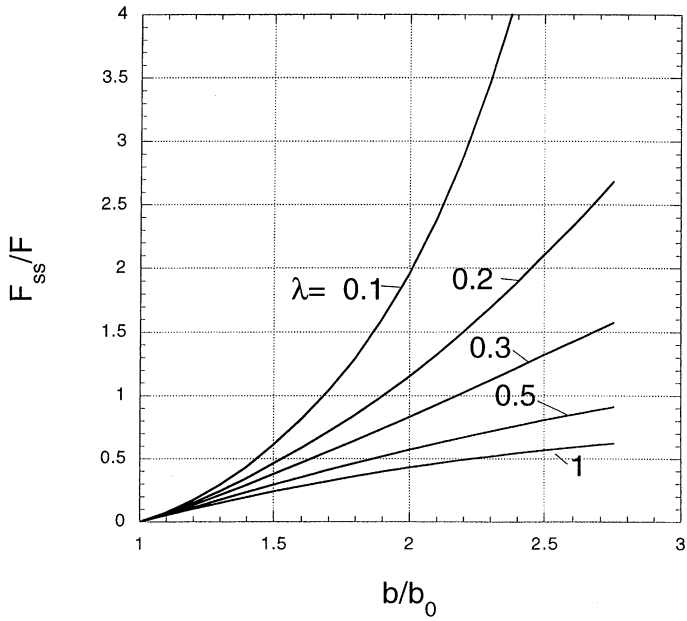

Fig. 3. Ratio of the mode-adjusted crack driving forces on the sides and curved front for a straight-sided blister on a flat substrate. Above a critical size, propagation on the curved front is favored over that on the straight sides, depending on the parameter λ specifying the mode dependence of the interface toughness.

substrate will be considered, followed by circumferentially propagating delaminations in Section 4. The four delamination cases to be studied are depicted in Fig. 4. Behaviors and some implications will be summarized in the concluding section.

2. Governing equations and two elementary results

2.1. Governing equations

In the undeformed reference state, the film is a thin cylindrical shell with radius R and thickness t. It is subject to a uniform, equi-biaxial compressive pre-stress σ_0. The displacement of the middle surface of the film has tangential components, $u_a(x_1,x_2)$, and outward normal component, $w(x_1,x_2)$, where $x_1 = x$ is the axial coordinate and $x_2 = y$ is the circumferential coordinate. The Donnell–Mushtari–Vlasov shell equations are used to described the debonded film. These equations, which generalize the von Karman plate equations to include shell curvature, are accurate for the so-called shallow deformation modes wherein the wavelength of the deformation mode is short compared to R. They apply to the two classes of modes analyzed here. The equations are as follows. The relations between the additional strains (in addition to the pre-strains)

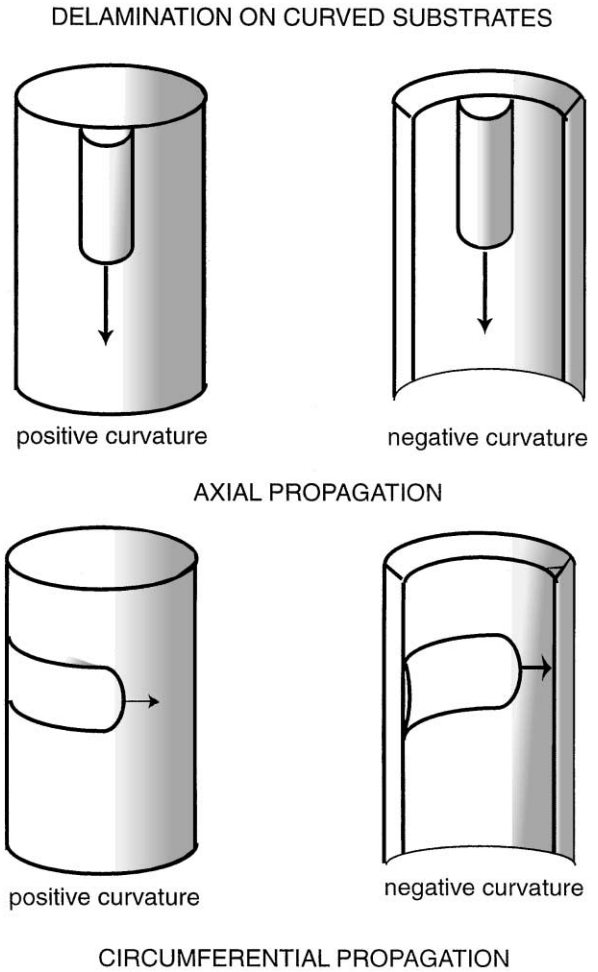

Fig. 4. Four types of straight-sided blisters considered in this paper.

and the displacements are (Sanders, 1963)

$$\varepsilon_{\alpha\beta} = (u_{\alpha,\beta} + u_{\beta,\alpha})/2 + b_{\alpha\beta}w + w_{,\alpha}w_{,\beta}/2 \quad (b_{11} = b_{12} = b_{21} = 0, b_{22} = 1/R), \tag{7}$$

$$\kappa_{\alpha\beta} = w_{,\alpha\beta},$$

where $\kappa_{\alpha\beta}$ are the bending strains. The stress–strain relations are

$$N_{\alpha\beta} = \frac{Et}{1-\nu^2}[(1-\nu)\varepsilon_{\alpha\beta} + \nu\varepsilon_{\gamma\gamma}\delta_{\alpha\beta}] - \sigma_0 t\delta_{\alpha\beta},$$

$$M_{\alpha\beta} = D[(1-\nu)\kappa_{\alpha\beta} + \nu\kappa_{\gamma\gamma}\delta_{\alpha\beta}], \qquad D = Et^3/[12(1-\nu^2)]. \tag{8}$$

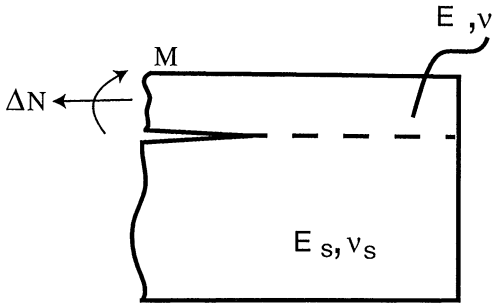

Fig. 5. Conventions for the local elasticity problem at the edge of the interface delamination.

Note that the resultant stresses, $N_{\alpha\beta}$, measure the total stress so that in the reference pre-stressed state $N_{\alpha\beta} = -\sigma_0 t\delta_{\alpha\beta}$. The bending moments, $M_{\alpha\beta}$, vanish in the reference state. The equilibrium equations are

$$N_{\alpha\beta,\beta} = 0,$$

$$M_{\alpha\beta,\alpha\beta} - N_{\alpha\beta}w_{,\alpha\beta} + N_{\alpha\beta}b_{\alpha\beta} = 0. \tag{9}$$

The boundary conditions along the edge of the blister are taken to be fully clamped: $w = u_1 = u_2 = w_{,\alpha}n_\alpha = 0$, where n_α is the outward normal to the edge.

The most important quantities from the solution to the problem for the deflected film for the purposes of determining the energy release rate and mode mixity at any point along the delamination edge are the local normal bending moment and normal resultant stress *change* (measured from the reference state):

$$M = M_{\alpha\beta}n_\alpha n_\beta$$

and

$$\Delta N = N_{\alpha\beta}n_\alpha n_\beta + \sigma_0 t. \tag{10}$$

The sign conventions for these quantities are indicated in Fig. 5. Both vanish in the reference state. The elasticity problem depicting the local loading along the delamination edge in Fig. 5 has been solved by Suo and Hutchinson (1990). Of interest here are the energy release rate

$$G = \frac{(1-\nu^2)\Delta N^2}{2Et} + \frac{6(1-\nu^2)M^2}{Et^3} \tag{11}$$

and the mode measure

$$\tan\psi = \frac{\sqrt{12}M + t\Delta N\tan(\omega)}{-\sqrt{12}M\tan(\omega) + t\Delta N}. \tag{12}$$

Here, it has been assumed that the second Dundurs elastic mismatch parameter, β_D, can be ignored and taken to be zero. Elastic mismatch influences ψ through ω which

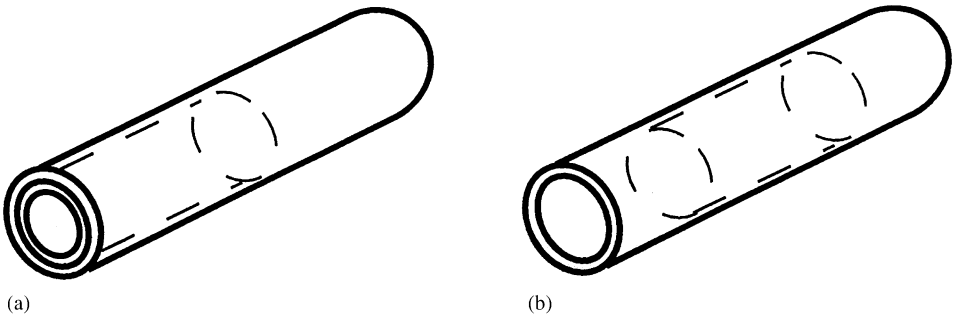

Fig. 6. Two elementary axisymmetric problems: (a) steady-state delamination propagation of an axially unconstrained film, and (b) steady-state delamination of a film constrained from net axial expansion.

depends on the first Dundurs parameter,

$$\alpha_D = \frac{E/(1-\nu^2) - E_2/(1-\nu_2^2)}{E/(1-\nu^2) + E_2/(1-\nu_2^2)}, \tag{13}$$

where E_2 and ν_2 are Young's modulus and Poisson's ratio of the substrate, respectively. Unless the mismatch is large, the influence of α_D is relatively weak (Hutchinson and Suo, 1992). For no mismatch ($\alpha_D = 0$), $\omega = 52.1^\circ$, which will be used to compute numerical results in this paper.

The energy release rate (11) neglects any inplane shear traction parallel to the crack edge, which induces a mode III component. The focus here will be on the sides of the straight-sided blister well behind the front, and on the center of the front itself, neither of which have a mode III component. The clamped conditions used at the delamination edges are an accurate approximation if there is no elastic mismatch or if the substrate material is stiffer than the film material. If, however, the film modulus is very large compared to that of the substrate, the fully clamped condition becomes a poor approximation (Cotterell and Chen, 2001). Then, the deformation of the substrate must be taken into account in setting the boundary conditions at the delamination edge.

2.2. Two elementary results

Consider the *unconstrained delamination of the film* propagating in steady-state along the cylinder as depicted in Fig. 6a, where the entire circumference of the film debonds. This is a simple axisymmetric problem. All the elastic energy stored in the film is released. By elementary energy accounting, the energy release rate is therefore

$$G_{ss} = \frac{1-\nu}{E}\sigma_0^2 t. \tag{14}$$

At the delamination edge, $\Delta N = \sigma_0 t$ and $M = \sqrt{(1-\nu)/[12(1+\nu)]}\sigma_0 t^2$. The expression for M at the delamination front has been obtained by solving the governing equations subject to axial symmetry and the clamped conditions, $w = w_{,x} = 0$, at the delamination

Table 1

v	ψ_{ss} (*unconstrained*)	ψ_{ss} (*constrained*)
0	-82.9°	-37.9°
1/5	-88.7°	-49.4°
1/3	(87.4°)	-57.3°
1/2	(82.1°)	-67.9°

edge. Substitution of ΔN and M into Eq. (11) gives Eq. (14), and substitution into Eq. (12) gives

$$\psi_{ss} = \frac{1 + \sqrt{(1+v)/(1-v)}\tan\omega}{-\tan\omega + \sqrt{(1+v)/(1-v)}}. \tag{15}$$

Numerical values of ψ_{ss} are given in Table 1. For $v = 1/5$ the crack tip has a very small positive value of mode I, but it is essentially subject to pure mode II (k_{II} is negative). For $v > 1/5$, the prediction from Eq. (15) is that there is a small negative value of K_I. This must be interpreted as a indication that the crack faces are in contact immediately behind the tip, and that the crack tip is in a state of pure mode II. Then, Eq. (14) remains valid if there are no frictional effects between the crack faces.

Next, consider the *constrained delamination of the film*. Suppose the film again completely debonds around the circumference but in such a way that the released film cannot expand axially. This would be the case if the axisymmetric interface crack propagated at two ends as in Fig. 6b. Now, if buckling does not occur, the conditions far behind the debond front are $\varepsilon_{xx} = 0$ and $N_{yy} = 0$. Together these imply $\Delta N = v\sigma_0 t$ and $M = \sqrt{(1-v^2)/12}\sigma_0 t^2$, where M is again obtained by solving the field equations subject to the clamped conditions at the delamination front (neglecting the buckling term, $N_{xx}w_{,xx}$). Substitution of these quantities into Eq. (11) and Eq. (12) gives

$$G_{ss} = \frac{1-v^2}{2E}\sigma_0^2 t \tag{16}$$

and

$$\psi_{ss} = \frac{\sqrt{(1-v^2)} + v\tan\omega}{-\sqrt{(1-v^2)}\tan\omega + v}. \tag{17}$$

The energy release rate (16) is precisely that for a film released subject to the plane strain constraint in the axial direction ($\varepsilon_{xx} = 0$). Table 1 gives ψ_{ss}. For this case, mixed mode conditions prevail with roughly equal proportions of modes I–II. The significant difference in mode mix at the delamination front in the two cases arises from the predominance of the inplane resultant stress change, ΔN, in the unconstrained case. It is physically intuitive that ΔN in Fig. 5 produces mode II conditions. By itself, without M, it produces a pure mode II loading and a closed crack tip. In the constrained case, ΔN is relatively small and M has a larger influence, leading to the roughly equal mix of modes I and II. For the problems analyzed below, the constrained case is the more relevant of the two, because conditions behind the front of a straight-sided blister experience a similar inplane constraint.

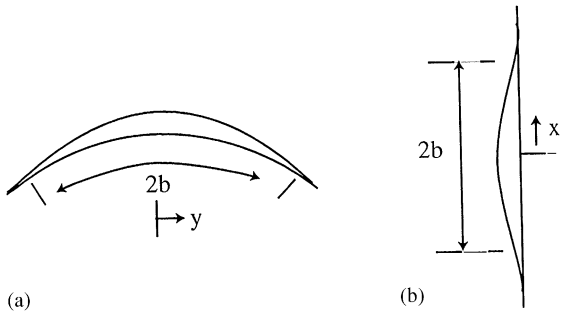

Fig. 7. Conventions for the one-dimensional analyses: (a) axial blister, and (b) circumferential blister.

3. Axial blisters

In this section, straight-sided blisters propagating in the axial direction are considered. The half-width of the blister is b and other features, including the positioning of the coordinates, are shown in Fig. 7a. We first carry out a one-dimensional analysis of the blister far behind the front to obtain the conditions on the sides. Then, we go on to make use of that result to compute the average energy release rate for the curved front.

3.1. One-dimensional analysis: behavior on the blister sides

Far behind the front, $u_1 = 0$, $u_2 = v(y)$, and $w(y)$. The governing field equations reduce to

$$Dw'''' - Nw'' + N/R = 0, \tag{18}$$

$$N' = 0, \tag{19}$$

where $(\ )' = \mathrm{d}(\ )/\mathrm{d}y$ and $N \equiv N_{22}$. The second of the two equilibrium equations implies that N is independent of y. The solution to Eq. (18) subject to symmetry about $y = 0$ and $w = w' = 0$ at $y = b$ is

$$w(y)/t = \eta\left[\frac{1}{2}\left(\left(\frac{y}{b}\right)^2 - 1\right) + \frac{1}{\pi\sqrt{n}\sin(\pi\sqrt{n})}(\cos(\pi\sqrt{n}y/b) - \cos(\pi\sqrt{n}))\right], \tag{20}$$

where

$$\eta = \frac{b^2}{Rt}$$

and

$$n = \frac{12(1-\nu^2)b^2}{\pi^2 E t^3}(-N). \tag{21}$$

In Eq. (20), n is as yet undetermined. It can be determined from the remaining conditions on $v(y)$: $v(0)=0$ (by symmetry) and $v(b)=0$ (clamped condition). The stress–strain equation in the circumferential direction implies $N=[Et/(1-\nu^2)]\varepsilon_{yy}-\sigma_0 t$ or, by Eq. (7),

$$N=[Et/(1-\nu^2)][v'+w/R+w'^2/2]-\sigma_0 t. \tag{22}$$

Integrate Eq. (22) from $y=0$ to $y=b$ using the conditions on $v(y)$ stated above to obtain

$$Nb=-\sigma_0 tb+[Et/(1-\nu^2)]\int_0^b [w/R+w'^2/2]\,\mathrm{d}y. \tag{23}$$

Carrying out the integrations in Eq. (23) using Eq. (20) and casting into dimensionless form, one obtains

$$\frac{n}{s}=1-\frac{\eta^2}{\pi^2 s}\left\{-2+\frac{3}{\sin^2(\pi\sqrt{n})}\left[1-\frac{\sin(2\pi\sqrt{n})}{2\pi\sqrt{n}}\right]\right\}, \tag{24}$$

where

$$s=\frac{12(1-\nu^2)b^2}{\pi^2 Et^2}\sigma_0. \tag{25}$$

Eq. (24) governs n. Only two dimensionless parameters specify the problem, s and η. The following connections will be useful in the sequel. Continue with the definition in Eq. (3) of b_0 as the half-width of the blister at the onset of buckling for a *flat substrate*. Moreover, note that the critical stress for the onset of buckling of a *flat* clamped plate of half-width b is $\sigma_c=\pi^2 Et^2/[12(1-\nu^2)b^2]$. Together, these two definitions imply that s can be expressed in either of two ways:

$$s=\left(\frac{b}{b_0}\right)^2=\frac{\sigma_0}{\sigma_c}. \tag{26}$$

Once n is determined, all the remaining details of the solution follow immediately. In particular, the energy release rate and mode mix along the sides of the blister are

$$\frac{G}{G_0}=\left[1-\left(\frac{n}{s}\right)\right]^2\left(1+\frac{1}{c^2}\right)$$

and

$$\psi=\frac{1+c\tan\omega}{-\tan\omega+c}, \tag{27}$$

where for $M>0$

$$c\equiv\frac{t\Delta N}{\sqrt{12}M}=\frac{\pi^2 s(1-(n/s))}{\sqrt{12}\eta(1-\pi\sqrt{n}\cot(\pi\sqrt{n}))}.$$

If $M<0$ (for negative curvature substrates), the film is considered to be on the underside of the substrate and the sign of c in Eq. (27) must be switched. The normalizing factor, G_0, in Eq. (27) continues to be defined by Eq. (2). The deflection at the center

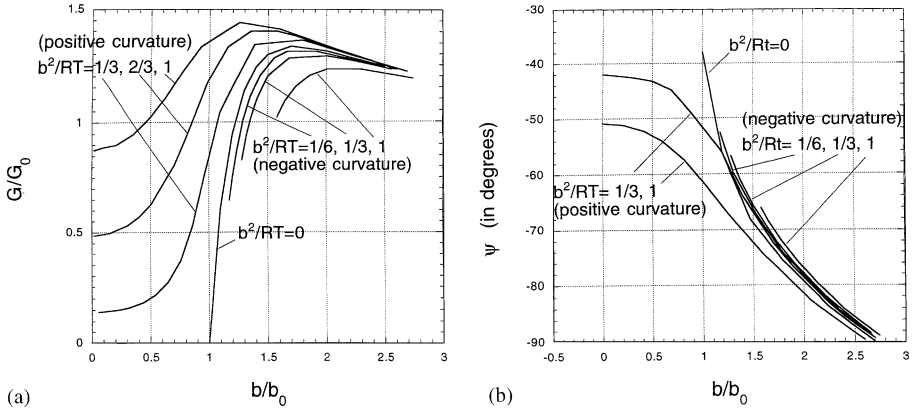

Fig. 8. Energy release rate (a) and mode mixity (b) along the sides of an axial blister.

of the blister is

$$w(0)/t = \eta\left[-\frac{1}{2} + \frac{1}{\pi\sqrt{n}\sin(\pi\sqrt{n})}(1-\cos(\pi\sqrt{n}))\right]. \tag{28}$$

It is positive for $n < 1$ and negative for $1 < n < 4$. The solutions having $n < 1$ are, therefore, associated with *positive curvature substrates*, while those having $1 < n < 4$ apply to *negative curvature substrates*. The dependencies of G and ψ on b/b_0 (c.f. Eq. (26)) are displayed in Fig. 8a and b for both positive and negative curvature substrates. With η specified, it is simplest to plot the curves by specifying values of n and then evaluating s trivially from Eq. (24). Also included are the curves for the flat substrate ($b^2/Rt=0$). The various curves have been plotted over the range in which each satisfies all the constraints required for a physically meaningful solution: (1) positive K_I; (2) one-signed deflection w consistent with either positive or negative substrate curvature; and (3) lower elastic energy in the deflected state than in the reference state (see Section 3.2).

The energy release rates for the positive curvature substrates are higher than that for the flat substrate at a given width, and they are significant at values of b/b_0 well below unity. The substrate curvature plays the role of an imperfection in the sense that, unlike that for the flat or negative curvature substrate, the problem is not a buckling problem, per se. Separations deflect away from the substrate producing stress intensities at even very low residual stress. The limit for G as $b \to 0$ from the present model is not physically correct. It is a result of using shell theory to model the film, which is necessarily limited to $b/t \gg 1$. Accurate results for very small widths would require a two-dimensional crack analysis.

Negative curvature substrates have delaminations with lower energy release rates than those for the flat substrate, but only slightly so. In this case, the delaminations all have $b/b_0 > 1$. Apart from their somewhat lower magnitudes, the energy release rates for negative curvature substrates are not appreciably different from their positive

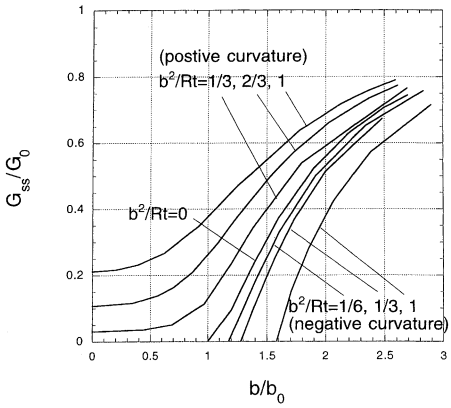

Fig. 9. Average steady-state energy release rate along the curve front of a straight-sided blister propagating in the axial direction.

curvature counterparts. The trends for the mode mix for these two types of substrates are also similar, with mode II becoming dominant as the width increases.

3.2. Steady-state propagation; behavior on the curved front

The average energy release rate on the curved front of a straight-sided blister propagating under steady-state conditions is the energy per unit width in the film in the undeflected state minus from the average energy per unit width in the deflected state far behind the front. The latter is evaluated using the solution produced in Section 3.1. A direct calculation of the difference between the two elastic energies gives

$$G_{ss} = \frac{1-\nu^2}{E}\frac{1}{b}\int_0^b [\sigma_0(N_{yy}+\sigma_0 t) + (N_{yy}+\sigma_0 t)^2/2]\,\mathrm{d}y - \frac{D}{2b}\int_0^b w''^2\,\mathrm{d}y, \tag{30}$$

where N_{yy} and w'' are given in Section 3.1. Evaluation of Eq. (30) gives

$$\frac{G_{ss}}{G_0} = \left(1-\left(\frac{n}{s}\right)^2\right) + \frac{12\eta^2}{\pi^4 s^2}\left[1 - \frac{\pi^2 n^2}{2\sin^2(\pi n)}\left(1+\frac{\sin(2\pi n)}{2\pi n}\right)\right]. \tag{31}$$

The results are plotted in Fig. 9. The result for a flat substrate coincides with Eq. (4), and this is also included in the figure. The spread in G_{ss} between positive and negative curvature substrates is even less than that for the energy release rate on the sides of the blister. As in that other case, the results become inaccurate when b becomes very small. The mode mixity on the front cannot be estimated by any equally simple procedure. It is expected to be roughly that presented for the flat substrate in Fig. 2.

4. Circumferential blisters

The conventions are shown in Fig. 7b. We first solve the problem for an axisymmetric blister of width $2b$. This problem represents the behavior of the propagating

straight-sided blister well behind the curved front and provides the results for the sides. Then, these results are used to determine the steady-state energy release rate for the curved front.

4.1. Axisymmetric analysis: behavior on the blister sides

The axisymmetric blister has $u_2 = 0$, $u_1 \equiv u(x)$ and $w(x)$. The solution is symmetric about $x=0$ with the clamped conditions at $x=b$: $u=w=w'=0$, where now $(\ )'=\mathrm{d}(\ )/\mathrm{d}x$. The governing equations reduce to

$$Dw'''' - Nw'' + Etw/R^2 + \nu N/R - (1-\nu)\sigma_0 t/R = 0, \quad N' = 0, \tag{32}$$

where now $N \equiv N_{11}$. The second of the equilibrium equations implies N is independent of x. Analogous to the step in the analysis of the axial blister, the conditions that u vanish at the ends of the interval provide the additional equation

$$N = -\sigma_0 t + [Et/((1-\nu^2)b)] \int_0^b [w'^2/2 + \nu w/R]\,\mathrm{d}x. \tag{33}$$

The definitions introduced for n, s, η, σ_c and b_0 in the previous section will all be retained, where now $N \equiv N_{11}$ in Eq. (21). The solution to the first of the equations in Eq. (32) is

$$w(x)/t = c_1 \cos(a_1 x/b) + c_2 \cos(a_2 x/b) + A, \tag{34}$$

where

$$A = \frac{\pi^2 s}{12(1+\nu)\eta} + \frac{\pi^2 \nu n}{12(1-\nu^2)\eta},$$

$$c_1 = \frac{-a_2 \sin(a_2) A}{a_2 \cos(a_1)\sin(a_2) - a_1 \sin(a_1)\cos(a_2)},$$

$$c_2 = \frac{a_1 \sin(a_1) A}{a_2 \cos(a_1)\sin(a_2) - a_1 \sin(a_1)\cos(a_2)},$$

$$(a_1, a_2) = \pi\sqrt{\tfrac{1}{2}n\{1 \pm \sqrt{1-\mu^2}\}}, \qquad \mu = 4\sqrt{3(1-\nu^2)}\eta n,$$

with the plus for a_1 and the minus for a_2. All quantities above will be real as long as $\mu < 1$, and this holds over nearly the entire solution space of interest. There is a small portion of the space wherein $\mu > 1$, and an alternative real representation has been used. The solution steps are essentially the same as those for $\mu < 1$ and in the interests of brevity will not be given.

Evaluation of Eq. (33) using Eq. (34) gives

$$\frac{n}{s} = 1 - \frac{12}{\pi^2 s}\left\{\frac{1}{4}B + \nu\eta\left(c_1 \frac{\sin a_1}{a_1} + c_2 \frac{\sin a_2}{a_2} + A\right)\right\}, \tag{35}$$

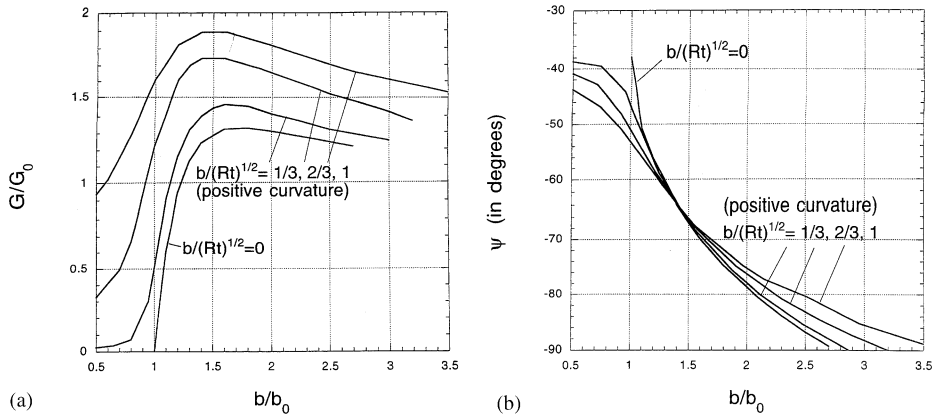

Fig. 10. Energy release rate (a) and mode mixity (b) along the sides of a circumferential blister. Only results for flat and positive curvature substrates are shown. ($v = 1/3$)

where

$$B = c_1^2 a_1^2 \left(1 - \frac{\sin(2a_1)}{2a_1}\right) + 2c_1 c_2 a_1 a_2 \left(\frac{\sin(a_1 - a_2)}{a_1 - a_2} - \frac{\sin(a_1 + a_2)}{a_1 + a_2}\right) + c_2^2 a_2^2 \left(1 - \frac{\sin(2a_2)}{2a_2}\right).$$

In addition to the parameters, s and η, this problem requires that Possion's ratio be specified. The numerical results presented below have been computed with $v = 1/3$. The deflection at the center of the blister is $w(0)/t = c_1 + c_2 + A$. The energy release rate and mode mixity along the sides of the blister are still given by Eq. (27), however, now for $M > 0$

$$c = \frac{\pi^2(n - s)}{\sqrt{12}[c_1 a_1^2 \cos a_1 + c_2 a_2^2 \cos a_2]}. \tag{36}$$

The first step in the procedure to produce numerical results is the generation of solutions to Eq. (35) for n. For any such n, the following conditions must be checked: a positive K_I, a one-signed deflection, and less elastic energy in the deflected state than in the reference state. If these are satisfied, the remaining quantities of interest are readily obtained. Plots of G/G_0 and ψ as a function of b/b_0 are given in Fig. 10. The same reference half-width, b_0, defined in Eq. (3) is used here. Each curve in Fig. 10 corresponds to *positive curvature substrates*, except the one for the flat substrate. Solutions for *negative curvature substrates* ($w(0) < 0$) were found, but in all cases the energy release rates were *far too small to be of physical interest*. As a practical matter, it appears that circumferential blisters are unlikely to form on negative curvature substrates. As in the case of the axial blister, the present case for positive

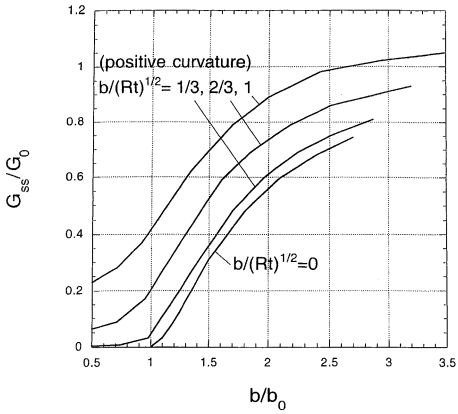

Fig. 11. Average steady-state energy release rate along the curve front of a straight-sided blister propagating in the circumferential direction. Only results for flat and positive curvature substrates are shown. ($\nu = 1/3$).

curvature substrates is not a bifurcation buckling problem, except in the limit of the flat substrate ($b/\sqrt{Rt} = 0$). A circumferential interface separation necessarily results in an outward deflection of the film away from the substrate when the curvature is positive. For negative curvature, the film remains pressed against the substrate.

The energy release rates for the positive curvature substrates are somewhat higher than those for the flat substrate, and they again occur at values of b/b_0 well below unity because the curvature plays the role of an imperfection for the separated film. The measure of mode mix on the circumferential blister sides in Fig. 10b shows that it is not significantly different from that for the flat substrates. Mode-dependent interface toughness is expected to provide the mechanism for arrest of the sides of the circumferential blisters.

4.2. Steady-state propagation; behavior on the curved front

The average steady-state energy release rate, G_{ss}, along the curved front of a straight-sided, circumferentially propagating blister is obtained by calculating the difference in the elastic energy in the film well ahead of the blister front and that well behind. The result of this calculation is

$$\frac{G_{ss}}{G_0} = 1 - \left(\frac{n}{s}\right)^2 + \frac{2E}{(1-\nu^2)\sigma_0^2 tb}\int_0^b [(1-\nu)t\sigma_0 w/R - Et(w/R)^2/2 - Dw''^2/2]\,\mathrm{d}x. \tag{37}$$

The Integral in Eq. (37) can be evaluated either analytically (the resulting expression is lengthy) or numerically. When cast in dimensionless form, the right hand side of Eq. (37) depends on n, s, η and ν. Numerical results for G_{ss}/G_0 as a function of b/b_0 are given in Fig. 11. They are roughly 20% higher than the corresponding quantities for the axially propagating blister.

5. Implications for blister propagation on curved substrates

A summary of the main findings is as follows:

(1) Conditions for the propagation of straight-sided delamination blisters extending circumferentially on negative curvature substrates are not favorable.

(2) Conditions are favorable for the propagation of straight-sided blisters in the axial direction on negative curvature substrates. The steady-state energy release rates are almost as large as those for propagation on positive curvature substrates.

(3) Interface separations on positive curvature substrates deflect away from the substrate even when they are small and do not require stresses to be at bucking levels. In this sense they act as an initial imperfection.

(4) The energy release rates for circumferentially propagating straight-sides blisters on a positive curvature substrate are somewhat larger than those for a axially propagating blister of comparable width. The mode mixity on the propagating fronts in these two cases are likely to be comparable, but trustworthy estimates are not available.

An interesting illustration of the phenomena investigated in this paper has been communicated privately to the author by M.D. Thouless. He reports that, when one soaks the label on a wine bottle to remove it, one almost always sees circumferential delaminations propagate from the edges of the label in the beginning stages of the removal process. The label swells as it absorbs water and develops inplane bi-axial compression, just as considered here. Intrigued by this effect, Thouless pasted labels on the inside of wide-mouth jars (the negative curvature case) and again observed their behavior when soaked in water. Now, only axially propagating delaminations were observed. The later observation is fully in accord with the present finding that circumferentially propagating blisters are energetically unfavorable on negative curvature substrates. The first of the observations might be explained by the fact that circumferentially propagating blisters have slightly larger energy release rates than their axial counterparts when the curvature is positive. However, the difference is not that large, and from the present study one could not argue that axially propagating blisters would not be observed.

Acknowledgements

This work has been supported in part by a grant entitled “Prime Reliant Coatings” from the Office of Naval Research, by the National Science Foundation (CMS-96-34632), and by the Division of Engineering and Applied Sciences, Harvard University.

References

Chai, H., Babcock, C.D., Knauss, W.G., 1981. One dimensional modeling of failure in aminated plates by delamination buckling. Int. J. Solids Struct. 17, 1069–1083.

Cotterell, B., Chen, Z., 2001. Buckling and cracking of thin films on compliant substrates under compression. Int. J. Fract., to be published.

Evans, A.G., Hutchinson, J.W., 1984. On the mechanics of delamination and spalling in compressed films. Int. J. Solids Struct. 20, 455–466.

Giola, G., Ortiz, M., 1997. Delamination of compressed thin films. Adv. Appl. Mech. 33, 120–192.

Hutchinson, J.W., Suo, Z., 1992. Mixed mode cracking in layered materials. Adv. Appl. Mech. 29, 64–191.
Hutchinson, J.W., Thouless, M.D., Lininger, E.G., 1992. Growth and configurational stability of circular, buckling-driven film delaminations. Acta Metall. Mater. 40, 295–308.
Nilsson, K.F., Giannakopoulos, A.E., 1995. A finite element analysis of configurational stability and finite growth of buckling driven delaminations. J. Mech. Phys. Solids 43, 1983–2021.
Nilsson, K.F., Thesken, J.C., Sindelar, P., Giannakopoulos, A.E., Storåkers, B., 1993. A theoretical and experimental investigation of buckling induced delamination growth. J. Mech. Phys. Solids 41, 749–782.
Sanders, J.L., 1963. Nonlinear theories for thin shells. Quart. Appl. Math. XXI (21), 34.
Suo, Z., Hutchinson, J.W., 1990. Interface crack between two elastic layers. Int. J. Fract. 43, 1–18.